Int J Appl Earth Obs Geoinformation 86 (2020) 102009

Contents lists available at ScienceDirect

Int J Appl Earth Obs Geoinformation

journal homepage: www.elsevier.com/locate/jag

Mapping wetland characteristics using temporally dense Sentinel-1 and Sentinel-2 data: A case study in the St. Lucia wetlands, South Africa

Bart Slagter[a,*], Nandin-Erdene Tsendbazar[a], Andreas Vollrath[b], Johannes Reiche[a]

[a] Wageningen University, Laboratory of Geo-Information Science and Remote Sensing, Droevendaalsesteeg 3, 6708PB Wageningen, the Netherlands
[b] European Space Agency, ESRIN, Via Galileo Galilei, Casella Postale 64, 00044 Frascati (RM), Italy

ARTICLE INFO

Keywords:
Wetland
Multi-level classification
Sentinel-1
Sentinel-2
Multi-sensor
Random forest

ABSTRACT

Wetlands have been determined as one of the most valuable ecosystems on Earth and are currently being lost at alarming rates. Large-scale monitoring of wetlands is of high importance, but also challenging. The Sentinel-1 and -2 satellite missions for the first time provide radar and optical data at high spatial and temporal detail, and with this a unique opportunity for more accurate wetland mapping from space arises. Recent studies already used Sentinel-1 and -2 data to map specific wetland types or characteristics, but for comprehensive wetland characterisations the potential of the data has not been researched yet. The aim of our research was to study the use of the high-resolution and temporally dense Sentinel-1 and -2 data for wetland mapping in multiple levels of characterisation. The use of the data was assessed by applying Random Forests for multiple classification levels including general wetland delineation, wetland vegetation types and surface water dynamics. The results for the St. Lucia wetlands in South Africa showed that combining Sentinel-1 and -2 led to significantly higher classification accuracies than for using the systems separately. Accuracies were relatively poor for classifications in high-vegetated wetlands, as subcanopy flooding could not be detected with Sentinel-1's C-band sensors operating in VV/VH mode. When excluding high-vegetated areas, overall accuracies were reached of 88.5% for general wetland delineation, 90.7% for mapping wetland vegetation types and 87.1% for mapping surface water dynamics. Sentinel-2 was particularly of value for general wetland delineation, while Sentinel-1 showed more value for mapping wetland vegetation types. Overlaid maps of all classification levels obtained overall accuracies of 69.1% and 76.4% for classifying ten and seven wetland classes respectively.

1. Introduction

During the last decades, wetlands have been determined as one of the most valuable ecosystems on Earth for both humanity and nature. It is assumed that their functions provide critical support for at least 7 of the 17 main Sustainable Development Goals as defined by the United Nations (Ramsar Convention, 2016). Depending on the wetland type, some important qualities of wetlands can be water storage and purification, shoreline protection, processing of carbon and other nutrients, food security and the support of a large biodiversity in plants and animals (Millennium Ecosystem Assessment, 2005; Ramsar Convention, 2016). Despite their importance, wetlands are currently being lost at a rate faster than any other ecosystem, mainly due to human activity (Millennium Ecosystem Assessment, 2005). To prevent further loss and implement and evaluate policy for preservation, large-scale monitoring and characterisation of different wetland types is of high importance.

Satellite-based remote sensing has been a widely adopted method for land cover mapping and monitoring in general, using both radar and optical data. However, accurately mapping wetlands is a challenging task when using satellite data (Gallant, 2015). Wetlands are usually not unified by a common land cover type or vegetation type, but only share the characteristic 'presence of water' either at the surface, below vegetation canopy or in the soil, which makes them difficult to delineate based on spectral or backscattering information (Gallant, 2015; Henderson and Lewis, 2008). Furthermore, such information may change during time due to the dynamics in flooding levels.

The capacities of most satellite sensors to cope with these wetland complexities are often insufficient. Although detecting large open waterbodies from space is usually easy, it gets challenging when flooding is present under a forest's canopy, when areas are surveyed that experience periods of persistent cloud-cover or when small or narrow wetlands need to be identified (Ozesmi and Bauer, 2002; Rosenqvist et al., 2007). The resolution of most satellite images is often too coarse for accurate detection. Satellites also need a short revisit time in order

* Corresponding author.
E-mail address: bartslagter94@gmail.com (B. Slagter).

https://doi.org/10.1016/j.jag.2019.102009
Received 16 July 2019; Received in revised form 4 October 2019; Accepted 1 November 2019
Available online 26 December 2019

to accurately detect flooding.

Another difficulty for large-scale wetland monitoring and characterisation is the lack of uniform and global wetland definitions (Amler et al., 2015) and comprehensive wetland classification schemes (Mahdavi et al., 2018). As a result, past studies have often narrowed down to specific aspects, such as a focus on characterising a certain wetland type (Rosenqvist et al., 2007), or on classifying a specific wetland characteristic (Semeniuk and Semeniuk, 1997). As a guideline for more comprehensive and generically applicable wetland classifications, two key characteristics are determined: wetland vegetation types and surface water dynamics (Keddy, 2010; Mitsch and Gosselink, 2015; Tiner, 1999).

Current developments within the Copernicus programme of the European Space Agency give a unique opportunity for more accurate wetland mapping from space, with its free access to high spatial and temporal resolution Sentinel-1 and Sentinel-2 data. The Sentinel-1 satellites carry a C-band (~5.5 cm wavelength) Synthetic Aperture Radar system, acquiring data in single- and dual-polarimetric modes with a 10-metre resolution (Torres et al., 2012). Radar remote sensing has proven to be a valuable mean for wetland mapping due to several advantages, namely weather- and daylight independence, sensitivity to water and moisture, and its ability to detect subcanopy water bodies (Henderson and Lewis, 2008). The Sentinel-2 satellites are equipped with a multispectral sensor, providing optical data in resolutions of 10-, 20- and 60 metres in the visible, near-infrared (NIR) and short-wave infrared (SWIR) portions of the electromagnetic spectrum (Drusch et al., 2012). Although optical remote sensing has limitations for wetland mapping when compared to radar, because clear-weather conditions and daylight are needed and subcanopy water body detection is not possible, optical data has proved its use as a complement besides radar data (Bourgeau-Chavez et al., 2009; Ozesmi and Bauer, 2002). As both these Sentinel missions comprise two polar-orbiting satellites and acquire images with relatively wide swaths, their revisit times – respectively five and six days for Sentinel-1 and -2 at the equator – are relatively high.

Several studies have already been done for wetland mapping and characterisation with the use of newly available Sentinel-1 and -2 data. Single-date wetland characterisations using Sentinel-2 (Araya-López et al., 2018; Bhatnagar et al., 2018; Kaplan and Avdan, 2017) and the combination of Sentinel-1 and -2 (Chatziantoniou et al., 2017; Kaplan and Avdan, 2018a; Whyte et al., 2018) already revealed the potential of the high spatial resolution of the data. Several attempts have also been done with multitemporal use of Sentinel-1 (Cazals et al., 2016; Huang et al., 2017; Kaplan and Avdan, 2018b; Mleczko and Mróz, 2018; Mróz et al., 2016; Muro et al., 2016; Tian et al., 2017; Tsyganskaya et al., 2018; Xing et al., 2018) and Sentinel-2 (Ludwig et al., 2019). Here, the value of temporally dense Sentinel-1 data was especially proved for accurately characterising surface water dynamics and flood frequencies in specific types of wetlands. Besides, these studies revealed a moderate potential for using Sentinel-1 for the detection of flooding in vegetated areas, which could not be done with optical data. The combination of Sentinel-1 and -2 data in multitemporal analyses has also been applied, although these studies have been limited to general wetland delineation (Hird et al., 2017) or used a non-globally transferable approach (Mahdianpari et al., 2018).

Most of these recent studies have looked at many wetland characteristics separately but did not investigate the potential of combining the temporally dense and high-resolution images of both Sentinel-1 and -2 for comprehensive wetland characterisations. As wetlands come in many different forms and can be characterised in different ways, it is necessary to consider characterisation methods that serve the needs of multiple users interested in different aspects of wetlands. It has been agreed that hierarchical and flexible wetland classification standards are preferred for future global wetland datasets (Hu et al., 2017). Current global land cover products such as the recently launched Copernicus Global Land Service (2019), which uses the ISO-certified United Nations Land Cover Classification System (Di Gregorio, 2005), have already focused on serving the needs of different user communities, but mapping wetland characteristics has remained limited here. In this broader context of large-scale mapping, there is a need to study the usability of Sentinel-1 and -2 for comprehensive wetland characterisations.

Here, we present a study on the use of the high-resolution and temporally dense Sentinel-1 and -2 data for wetland mapping within multiple levels of characterisation. We first designed a wetland classification scheme considering three key classification levels: general wetland delineation, wetland vegetation types and surface water dynamics. Then, we applied Random Forest classifications using several temporal metrics obtained from two years of satellite imagery and present results for the St. Lucia wetlands, South-Africa. We compared the classification accuracies for both satellite systems separately and combined to assess the potential of the data for applications in large-scale wetland monitoring.

2. Materials

2.1. Study area

The St. Lucia wetlands (also known as the iSimangaliso wetlands), located at the eastern shore of South Africa (Fig. 1), were used as a study area. The St. Lucia wetland system is a UNESCO World Heritage site and is an official Ramsar site. Being 1400 km^2 in size, it comprises the largest estuarine wetland system in Southern Africa (Perissinotto et al., 2013), where four large rivers enter the main water body of Lake St. Lucia. The area has a sub-tropical climate and annual precipitation

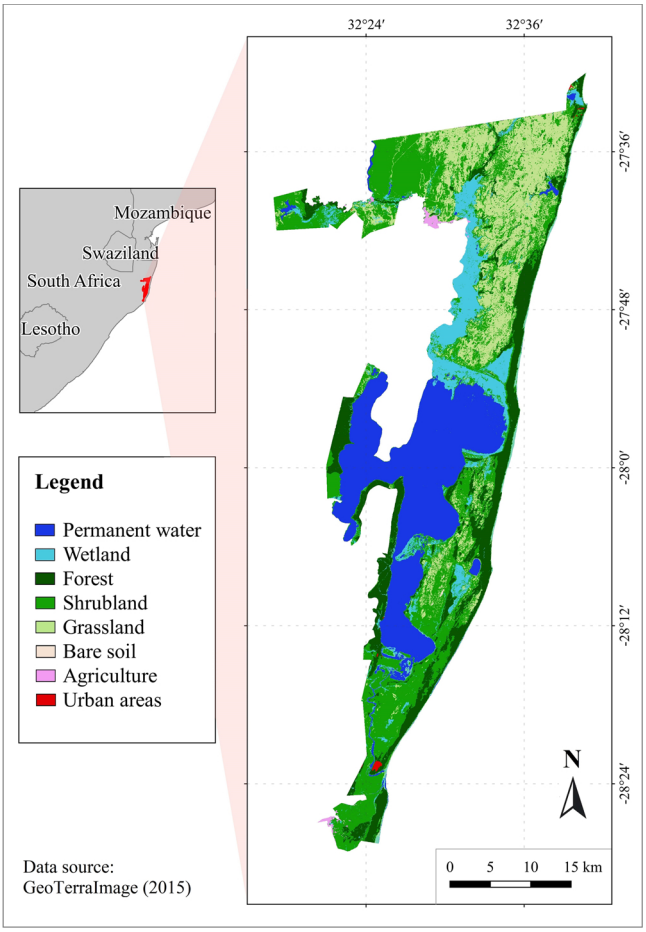

Fig. 1. Overview of the study area (land cover data source: GeoTerraImage, 2015).

varies from 1200 to 1300 mm (Bassa et al., 2016). The St. Lucia wetlands are characterised by a high diversity of ecosystems, including marine, inland lake, estuarine, forested dunes, mangrove, and coastal and swamp forest ecosystems (Adam and Mutanga, 2009). The area is also highly dynamic in terms of flooding levels. For these reasons, it was determined as a suitable study area for this research.

The St. Lucia wetlands were subject to severe droughts in 2015 and 2016 (iSimangaliso Wetland Park Authority, 2017). Therefore, more stable years were chosen to be used as a study period, namely from October 2016 until October 2018. This two-year period covers two cycles of wet seasons (usually from January – March) and dry seasons (usually from May – September), starting and ending in the transition between these extremes.

2.2. Data

Sentinel-1 and -2 satellite images covering the period from October 2016 to October 2018 were sourced from the cloud-based geospatial processing platform Google Earth Engine (GEE) (Gorelick et al., 2017). The Sentinel-1 data provided within GEE is Ground Range Detected, acquired in dual-polarimetric (VV/VH) Inferometric Wide Swath mode and pre-processed as a Level-1 data product. Within the study area and time period, a total of 65 Sentinel-1A images were selected (complemented with several additional images to cover small areas on the northern edge of the study area) with a 12-day revisit time. Sentinel-2 data is provided in GEE as a Level-1C product representing Top of Atmosphere reflectance. Only images with a cloud-cover less than 40% were selected, resulting in a time series of 286 Sentinel-2 images from tiles T36JVP and T36JVQ.

3. Methods

A full overview of the methodological flow chart can be found in Fig. 2 and is discussed in detail in the following subsections. First, pre-processing of the Sentinel-1 and -2 images was done (Section 3.1). Five temporal metrics were calculated from a set of relevant variables. Then, several Random Forest classifications (Breiman, 2001) were done using training points sampled from the study area (Section 3.2). Finally, all classifications were validated with an independent validation dataset (Section 3.3).

3.1. Data pre-processing

Within GEE, Sentinel-1 images are pre-processed into an analysis-ready format using border noise removal, thermal noise removal, radiometric calibration and orthorectification (Google, 2018a). Further pre-processing included the correction of radiometric distortions along terrain slopes (Hoekman and Reiche, 2015) using the 30-metre resolution digital elevation model from the Shuttle Radar Topography Mission (Farr et al., 2007) and the removal of speckle noise using the Extended Lee Sigma Filter with a window size of 7 × 7 pixels (Lee et al., 2015).

The Sentinel-2 images were further pre-processed within GEE to remove cloud- and cirrus-cover, using the provided QA-bands. Additional masking was done by using threshold values for Band 2 (for additional removal of dense clouds) and Band 10 (for additional removal of cirrus clouds). In order to obtain a cloud-free time series, eight quarterly median composites were produced over the two-year time period, of which the first (October, November and December 2016) had to be removed due to persistent cloud-cover during this quarter.

From each image within the time series of Sentinel-1 and -2, respectively three and two variables were obtained, as described in Table 1. From these variables, several temporal metrics – the mean, median, maximum, minimum and standard deviation – were calculated within GEE over the entire time period. A stacked GeoTiff image was exported with these 25 temporal metrics stored as separate bands.

3.2. Classification

3.2.1. Multi-level classification scheme

A multi-level classification scheme was designed based on three levels (Fig. 3). One level for general wetland delineation and two subsequent levels for classifying the most important wetland characteristics as determined by Keddy (2010), Mitsch and Gosselink (2015) and Tiner (1999): wetland vegetation types and surface water dynamics.

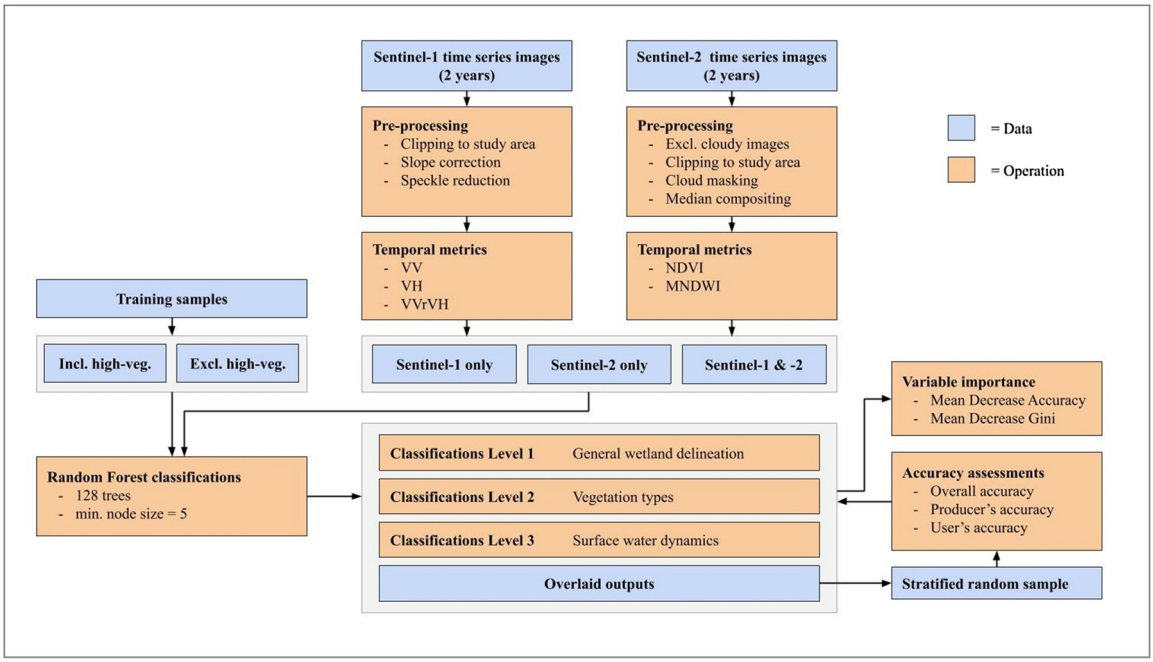

Fig. 2. Overview of the methodology used in this study (for abbreviations of temporal metrics, see Table 1).

Table 1
Overview of Sentinel-1 and -2 variables used for this study.

Satellite	Variable	Description	Equation
Sentinel-1	VV	Backscattering value (γ°_{flat}) for vertically polarised transmit and vertically polarised receive.	*NA*
	VH	Backscattering value (γ°_{flat}) for vertically polarised transmit and horizontally polarised receive.	*NA*
	VVrVH	Ratio to indicate the VV backscattering relative to the VH backscattering.	$VVrVH = \frac{VV}{VH}$
Sentinel-2	NDVI	Normalised Difference Vegetation Index: indicates the occurrence of vegetation based on the normalised difference in NIR (Band 8) and red (Band 4) reflectance (Kriegler et al., 1969).	$NDVI = \frac{NIR - Red}{NIR + Red}$
	MNDWI	Modified Normalised Difference Water Index: indicates the occurrence of water bodies based on the normalised difference in green (Band 3) and SWIR (Band 11) reflectance (Xu, 2006)	$MNDWI = \frac{Green - SWIR}{Green + SWIR}$

For mapping wetlands in highly vegetated areas, the observation of double-bounce scattering during flooding is needed, which requires a certain level of vegetation penetration of a radar sensor. In high-vegetated wetlands such as mangrove- or swamp forests, this is best achieved with high-wavelength L- or P-band sensors and HH mode, although varying results have also been achieved with C-band and VV mode (Wang et al., 1995). For this study it was expected that the C-band sensors, operating in VV/VH mode, aboard the Sentinel-1 satellites had only moderate capabilities to map high-vegetated wetlands, and therefore two different sets of classifications were done: one including high-vegetated wetlands (+HV) and one excluding high-vegetated wetlands (-HV), considering in total ten and seven wetland classes respectively (Fig. 3). Both classification sets were done using Sentinel-1 only (S1), Sentinel-2 only (S2) and the combination of Sentinel-1 and -2 (S1S2).

In Level 1 *upland* comprises all terrestrial land cover types (e.g. forests, grasslands, urban areas, agricultural land, bare soil) and *permanent water* comprises all areas that are covered with water at least 80% of time. *Wetlands* are all areas in between these definitions of upland and permanent water. The used class definitions for Level 2 and Level 3 are described in Table 2. To delineate the used vegetation classes, thresholds were adopted from the National Vegetation Classification Standard (Federal Geographic Data Committee, 1997). Examples of each wetland class within the study area displayed in high-resolution aerial images can be found in Fig. 4.

3.2.2. Training data

Several global, regional and local data products were used as a reference to acquire training data for the defined wetland classes (Table 3). Only areas where multiple sources pointed out the occurrence of a wetland area, a certain wetland vegetation class and a certain type of surface water dynamics were appointed as a suitable training sample. Within these areas, the temporal metrics were sampled with 400 random points per class in Level 1 and 200 random points per class in Level 2 and Level 3.

3.2.3. Random Forest classification

All classifications were done within R (R Core Team, 2018) using Random Forests, a non-parametric supervised machine learning algorithm (Breiman, 2001). Random Forests have proven their use for classifications with the large amounts of data in satellite images, mainly because they can handle the large differentiation within land cover classes and noise data can be neutralised (Rodriguez-Galiano et al., 2012).

The temporal metrics derived from the sample points were used as input variables for the Random Forests. The number of trees in each Random Forest classification was set to 128, which is determined to be an optimal number in the consideration between accuracy and processing speed (Oshiro et al., 2012). The minimum node size was set to 5 to limit the tree depth. To evaluate the importance of the individual metrics, their Mean Decrease in Accuracy (MDA) and Mean Decrease in Gini (MDG) were computed for each classification.

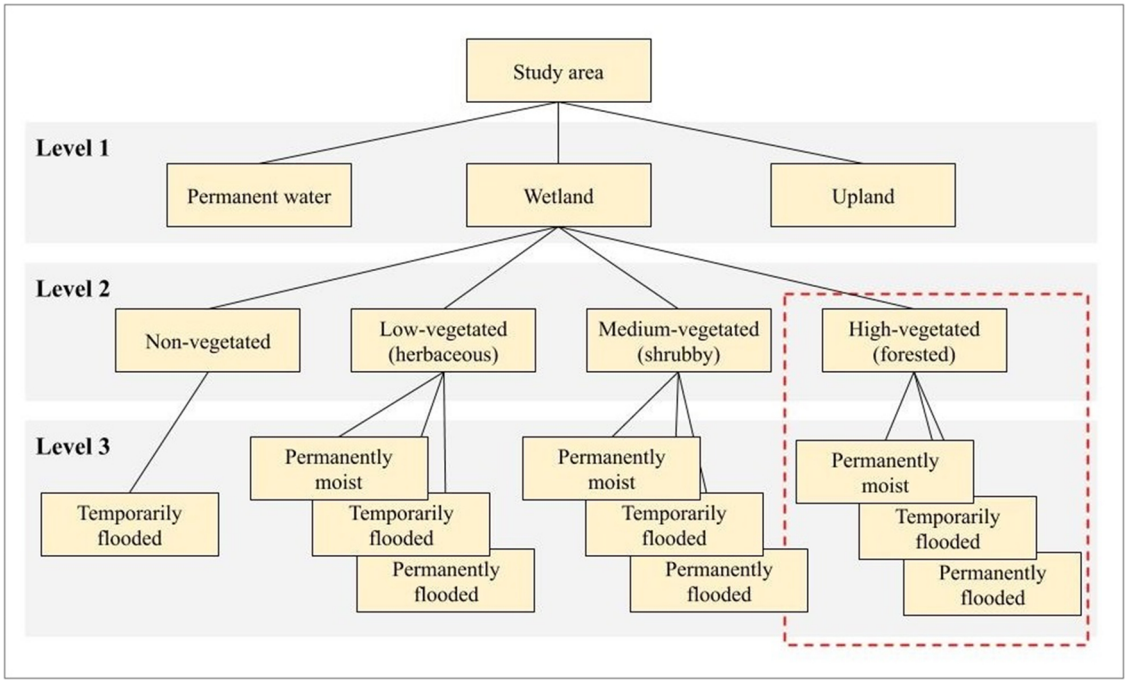

Fig. 3. Multi-level wetland classification scheme designed for this study.

Table 2
Definitions of the considered classes for wetland characterisations in Level 2 and Level 3.

Level	Class	Description	Thresholds
Level 2 (wetland vegetation types)	Non-vegetated	Wetlands with no or sparse vegetation, such as tidal flats.	< 10% vegetation cover.
	Low-vegetated (herbaceous)	Wetlands such as low-vegetated marshes, with herbaceous vegetation without significant woody tissue.	< 0.5 metre in height. < 25% shrub- or forested cover.
	Medium-vegetated (shrubby)	Wetlands such as higher-vegetated marshes, with shrubby vegetation or a bushy appearance.	> 0.5 metre in height. > 25% shrubby cover.
	High-vegetated (forested)	Wetlands such as swamp- or mangrove forests, covered by trees with a single main stem and a definite crown.	> 5 metre in height. > 25% forested cover.
Level 3 (surface water dynamics)	Permanently moist	Wetlands that have a constant occurrence of low amounts of water, but do not experience severe flooding.	Flooded: < 20% of time.
	Temporarily flooded	Wetlands that are subject to severe flooding with high amounts of water.	Flooded: > 20% of time and < 80% of time.
	Permanently flooded	Vegetated wetlands that are constantly or nearly constantly flooded with high amounts of water.	Flooded: > 80% of time. > 10% vegetation cover.

The results in the Level 1 classification were post-classified by removing all isolated pixel clumps (containing 3 pixels or less in eight directions) and replacing them by the majority pixel value of its direct neighbours in a 3 × 3 window. The post-classified outputs from Level 1 were used as inputs for the Level 2 and Level 3 classifications, where upland and permanent water were masked out. The non-masked areas – the wetlands – were then further classified for their vegetation types (Level 2) and surface water dynamics (Level 3). The output maps from all levels were overlaid, in order to obtain final maps considering all combinations of wetland classes.

3.3. Validation

For validation data collection, the overlaid classification output that included all ten wetland classes (+HV) and had the lowest out-of-bag error was used as a stratification. For each class represented in the stratification, 50 sample points were collected per stratum. All validation points were visually assessed and appointed to a class in each

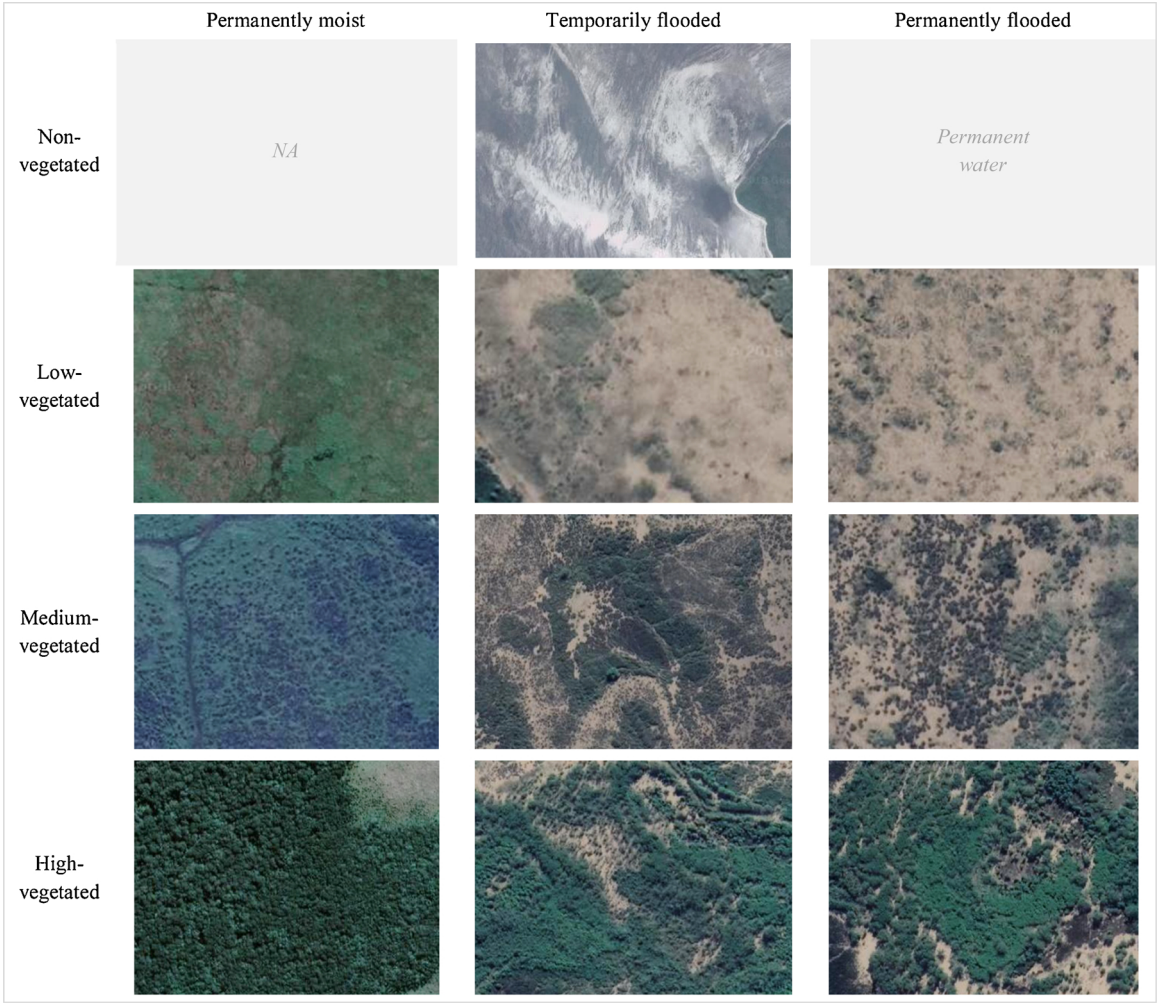

Fig. 4. Aerial images of examples of wetland classes. Images in the class 'temporarily flooded' were taken during a flood event. Brownish colours indicate the occurrence of water (Google, 2018b).

Table 3
Overview of the used reference data. The classification level for which each dataset was consulted is stated under 'Level'.

Dataset	Description	Author/reference	Level
Global scale			
Global Surface Water Dataset	30-metre resolution map of global dynamics in surface water from 1984–2015.	Pekel et al. (2016)	1, 3
Google Earth images	High-resolution global composition of aerial- and satellite images in different scales and from different dates.	Google (2018b)	1, 2, 3
Microsoft Bing Maps images	High-resolution global composition of aerial- and satellite images in different scales.	Microsoft Bing Maps (2018)	1, 2
PALSAR-2 Global 25 m Resolution Mosaic	25-metre resolution HH and HV L-band radar image from the ALOS PALSAR-2 satellite sensor, acquired in 2017.	Shimada et al. (2014)	1, 2
Planet Explorer satellite images	3-metre resolution global composition of multitemporal satellite images.	Planet (2018)	1, 3
Shuttle Radar Topography Mission	30-metre resolution global digital elevation model.	Farr et al. (2007)	1
Tropical & Subtropical Wetland Distribution	231-metre resolution classification of wetland types in tropical and sub-tropical regions.	Gumbricht et al. (2017)	1, 2
Regional scale			
KwaZulu-Natal Land Cover	20-metre resolution land cover classification of the KwaZulu-Natal region in South-Africa.	Ezemvelo KZN Wildlife (2011)	1
NFEPA Wetlands	Vector map with classifications of wetland types in South Africa.	Nel et al. (2011)	1, 2
NFEPA Wetland Vegetation	Vector map with classifications of wetland vegetation types in South Africa.	Nel et al. (2011)	2
South African aerial photography	0.5-metre resolution aerial photography of South Africa.	National Geospatial Information (2018)	1, 2
South African Land Cover Dataset	30-metre resolution land cover classification of South Africa	GeoTerraImage (2015)	1, 2
Vegetation Map of South Africa, Lesotho and Swaziland	Vector map with classifications of general vegetation types in South Africa.	Mucina et al. (2006)	2
Local scale			
Local study	Land cover classification of the Mfabeni mire site within the St. Lucia wetlands.	Clulow et al. (2013)	1, 2
Local study	Vegetation type classification in the surroundings of the St. Lucia village.	Lück-Vogel et al. (2016)	1, 2
Local study	Land cover classification in the entire area of the St. Lucia wetlands.	Maseko et al. (2017)	1
Local study	Land cover classification in the entire area of the St. Lucia wetlands.	Whyte et al. (2018)	1, 2

classification level. The reference data sources as described in Table 3 were consulted for this procedure. After the production of this validation dataset, confusion matrices were generated for all classifications and the overall accuracy (OA), producer's accuracy (PA) and user's accuracy (UA) were calculated.

4. Results

Among the +HV classifications, the lowest out-of-bag errors were observed for the S1S2 classifications. Therefore, the overlaid output from these classifications was used as stratification to create the validation dataset (Fig. 6). Accuracy overviews of all level-based classifications and the overlaid outputs can be found in Tables 4 and 5 respectively. Fig. 5 shows the relative importance of the used temporal metrics per classification. Fig. 7 shows the full output of the most accurate classification ($S1S2_{-HV}$) and a detailed comparison with the other classification outputs.

The OAs for classifications in Level 1 (general wetland delineation) ranged from 73.7%–88.5% (Table 4). The OA of $S2_{+HV}$ (80.2%) was relatively high compared with the OA of $S1_{+HV}$ (73.7%). $S1S2_{+HV}$ showed an improvement of the OA to 84.3%. In terms of specific classes, *wetland* was classified with relatively high accuracies, while accuracies for *upland* were relatively low. These classes showed a high confusion throughout all classifications especially in high-vegetated areas. The exclusion of high-vegetated wetlands led to relatively higher OAs, leading to 88.5% for $S1S2_{-HV}$. Especially the accuracies for *upland* improved. A high confusion was also observed in both Sentinel-1 classifications for *permanent water* and *wetland,* especially in shallow water areas, where *permanent water* was overestimated. The standard deviations for MNDWI and VV as well as the maximum NDVI showed to

Table 4
Overview of the accuracies (%) of the classifications in each level.

	$S1_{+HV}$		$S2_{+HV}$		$S1S2_{+HV}$		$S1_{-HV}$		$S2_{-HV}$		$S1S2_{-HV}$	
Level 1	OA:	**73.7**	OA:	**80.2**	OA:	**84.3**	OA:	**80.3**	OA:	**85.8**	OA:	**88.5**
	PA	UA	PA	UA	PA	UA	PA	UA	PA	UA	PA	UA
Permanent water	94.2	62.0	88.5	93.9	88.5	88.5	92.3	63.2	90.4	94.0	94.2	75.4
Upland	57.3	49.6	66.1	54.7	44.4	80.9	79.0	69.5	84.7	69.5	82.3	85.0
Wetland	75.9	85.2	83.3	88.0	95.5	84.4	78.9	89.9	85.5	92.3	89.9	92.4
Level 2	OA:	**83.8**	OA:	**77.0**	OA:	**90.9**	OA:	**87.6**	OA:	**79.5**	OA:	**90.7**
	PA	UA	PA	UA	PA	UA	PA	UA	PA	UA	PA	UA
Non-vegetated	100.0	75.0	95.6	93.5	100.0	100.0	100.0	76.9	95.6	95.6	100.0	100.0
Low-vegetated	84.3	92.9	70.5	75.4	93.3	92.7	84.7	91.7	73.2	79.5	90.7	90.7
Medium-vegetated	80.0	78.6	67.5	71.4	85.0	86.9	89.2	85.1	80.2	73.8	88.4	88.4
High-vegetated	84.9	77.6	96.7	78.1	91.6	89.4	*NA*	*NA*	*NA*	*NA*	*NA*	*NA*
Level 3	OA:	**75.4**	OA:	**75.6**	OA:	**82.0**	OA:	**77.8**	OA:	**76.0**	OA:	**87.1**
	PA	UA	PA	UA	PA	UA	PA	UA	PA	UA	PA	UA
Permanently moist	73.0	73.0	66.2	77.8	83.9	83.2	75.6	90.0	72.4	79.3	94.1	87.8
Temporarily flooded	64.1	81.2	72.3	87.3	73.5	93.2	66.7	77.9	68.4	87.4	78.4	94.0
Permanently flooded	97.6	71.3	90.8	60.3	98.9	67.4	96.1	77.9	93.6	62.9	94.9	78.1

Table 5
Overview of the accuracies (%) of the overlaid level outputs. NV = non-vegetated, LV = low-vegetated, MV = medium-vegetated, HV = high-vegetated, PM = permanently moist, TF = temporarily flooded, PF = permanently flooded.

Overlaid maps	$S1_{+HV}$		$S2_{+HV}$		$S1S2_{+HV}$		$S1_{-HV}$		$S2_{-HV}$		$S1S2_{-HV}$	
	OA: PA	**55.0** UA	OA: PA	**55.5** UA	OA: PA	**69.1** UA	OA: PA	**64.9** UA	OA: PA	**64.1** UA	OA: PA	**76.4** UA
Permanent water	94.2	62.0	88.5	93.9	94.2	98.0	92.3	63.2	90.4	94.0	94.2	75.4
Upland	58.1	49.7	66.9	54.6	36.3	90.0	79.0	69.5	85.5	69.7	83.1	84.4
$WL_{NV\ TF}$	37.5	64.3	89.5	82.7	97.9	94.0	41.7	64.5	89.6	86.0	64.6	91.2
$WL_{LV\ PM}$	63.2	66.7	29.8	54.8	77.2	88.0	61.4	71.4	40.4	54.8	73.7	77.8
$WL_{LV\ TF}$	51.9	84.8	46.3	59.5	79.6	86.0	61.1	71.7	37.0	52.6	77.8	82.4
$WL_{LV\ PF}$	90.7	86.7	79.1	72.3	95.3	82.0	93.0	86.9	76.7	71.7	95.3	80.4
$WL_{MV\ PM}$	38.2	34.2	32.4	40.7	82.4	56.0	32.4	28.9	29.4	55.6	76.5	53.1
$WL_{MV\ TF}$	18.5	50.0	21.5	34.1	55.4	72.0	26.2	44.7	30.8	42.6	44.6	69.0
$WL_{MV\ PF}$	88.9	51.6	66.7	41.4	88.9	64.0	86.1	64.6	75.0	38.6	80.6	64.4
$WL_{HV\ PM}$	3.3	20.0	30.0	36.0	50.0	30.0	*NA*	*NA*	*NA*	*NA*	*NA*	*NA*
$WL_{HV\ TF}$	56.5	34.2	45.7	45.7	52.2	48.0	*NA*	*NA*	*NA*	*NA*	*NA*	*NA*
$WL_{HV\ PF}$	36.4	36.4	54.5	20.0	100.0	22.0	*NA*	*NA*	*NA*	*NA*	*NA*	*NA*

be important metrics in this classification level (Fig. 5).

The OAs for classifications in Level 2 (wetland vegetation types) ranged from 77.0%–90.9% (Table 4). The OA of $S1_{+HV}$ (83.8%) was relatively high compared with the OA of $S2_{+HV}$ (77.0%). A high accuracy improvement was observed in $S1S2_{+HV}$, leading to an OA of 90.9%. *Non-vegetated wetland* was classified with relatively high accuracies especially in classifications involving Sentinel-2, while *low-, medium-* and *high-vegetated wetland* had relatively high accuracies in classifications involving Sentinel-1. *Medium-vegetated wetland* had the highest confusion throughout all classifications, both with *low-vegetated-* and *high-vegetated wetland.* The two S1 classifications showed a relatively poor distinction for the classes *non-vegetated-* and *low-vegetated wetland,* resulting in an overestimation of *non-vegetated wetland.* The exclusion of high-vegetated wetlands led to small OA improvements in $S1_{-HV}$ and $S2_{-HV}$, but not in $S1S2_{-HV}$. Important metrics in this classification level were the median and minimum MNDWI, mean VH and minimum VV (Fig. 5).

The OAs for classifications in Level 3 (surface water dynamics) ranged from 75.4%–87.1% (Table 4). The OAs for $S1_{+HV}$ and $S2_{+HV}$ showed no significant difference, but the improvement in $S1S2_{+HV}$ was relatively high, leading to an OA of 82.0%. The exclusion of high-vegetated wetlands led to a significant OA increase only in $S1S2_{-HV}$ (87.1%). An overestimation of *permanently flooded wetland* at the cost of *temporarily flooded wetland* was indicated by their high PA and UA respectively. Important metrics in this classification level were the maximum MNDWI and the mean and median VVrVH (Fig. 5).

By overlaying the level-based classification outputs, multi-level wetland maps were revealed (Fig. 7). The OAs of these maps showed no significant differences for the S1 and S2 classifications (Table 5). The results obtained in both S1S2 classifications showed large accuracy improvements though, with an OA of 76.4% for $S1S2_{-HV}$. Several classes were occasionally severely over- or underestimated.

5. Discussion

The results for the wetland characterisation methods showed the superiority of combining Sentinel-1 and -2 data over the use of data from the individual satellites. Also, it was found that the use of Sentinel-1 data did not suffice for accurate wetland delineations and classifications in highly vegetated areas. Classifications neglecting high-vegetated wetlands resulted in higher accuracies.

The Level 1 classifications for general wetland delineation showed satisfying accuracies for Sentinel-2 and the combined use of Sentinel-1 and -2, while the sole use of Sentinel-1 performed relatively poor (Table 4). The observation of Sentinel-2 being more accurate for general wetland delineation than Sentinel-1 is in line with the findings in earlier studies (Hird et al., 2017; Mahdianpari et al., 2018). Confusion in all classifications was observed mainly between *wetland* and *upland*.

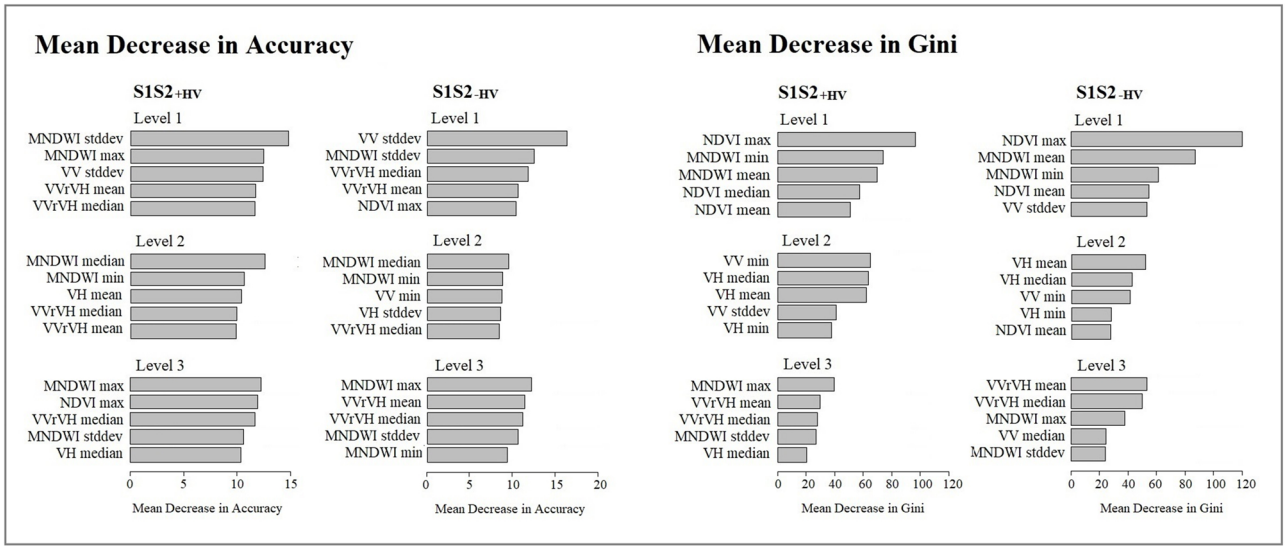

Fig. 5. Indicators for variable importance of the top-5 ranked metrics according to their MDA and MDG scores.

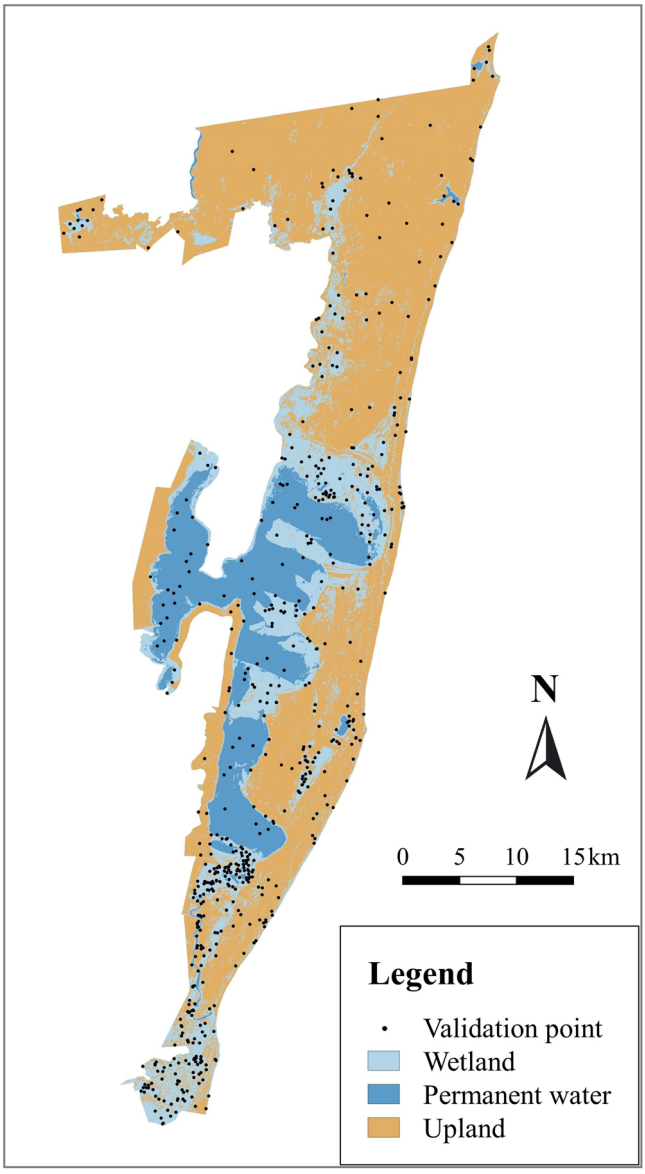

Fig. 6. Distribution of validation points generated with a stratified random sample from the $S1S2_{+HV}$ classification. The background map shows the Level 1 classification result for $S1S2_{+HV}$.

These errors were largely reduced after the exclusion of high-vegetated areas. This can be partially explained by a limited capacity of Sentinel-1's C-band sensors operating in VV/VH mode to capture differences in upland forests and high-vegetated wetlands such as swamp- or mangrove forests. Such findings were also achieved by Mahdianpari et al. (2018). As earlier studies revealed, the use of L- or P-band radar systems and HH polarisation is more suitable for this purpose (Wang et al., 1995). A clear difference for the classifications with either Sentinel-1 or -2 is the amount of confusion between *permanent water* and *non-vegetated wetland*, where Sentinel-1 showed a poorer performance than Sentinel-2. This indicates that Sentinel-2 has a higher capacity to capture differences in areas that are on the edge of being either shallow water or tidal flat, as such differences are rather distinguishable in terms of spectral reflectance than in terms of structure.

The Level 2 classifications for wetland vegetation types showed higher accuracies for Sentinel-1 than for Sentinel-2. The accuracy improvement when combining Sentinel-1 and -2 was relatively high (Table 4). The ordinal nature of the used classification scheme explains the confusion observed for *medium-vegetated wetland,* as this class falls in between *low-* and *high-vegetated wetland*. This phenomenon is known for shrubland classes within vegetation classifications in general (Tsendbazar et al., 2016). As the importance of the metrics VH mean and VV minimum was high, it is likely that volume scattering (especially for VH in *medium-* and *high-vegetated wetland*), double-bounce scattering (especially for VV in *low-* and *medium-vegetated wetland*) and specular reflection (especially for VV in *non-* and *low-vegetated wetland*) are well observed with Sentinel-1 and contribute to an accurate classification of wetland vegetation types. The addition of Sentinel-2, especially the metrics for MNDWI, clearly leads to a more accurate distinction of *non-* and *low-vegetated wetland*.

The Level 3 classifications for surface water dynamics showed similar overall accuracies for Sentinel-1 and -2, but the combination of Sentinel-1 and -2 led to a high accuracy improvement (Table 4). The similar accuracies for Sentinel-1 and -2 are somewhat surprising, as it was expected that Sentinel-1 and its high-temporal density would outperform Sentinel-2 for mapping wetland dynamics. However, this can be explained by the fact that the used temporal metrics were derived from the entire time period, leading to compressed information on temporal dynamics. Also, only three classes for surface water dynamics were considered, while Sentinel-1's quality can be truly emphasised in more detailed classifications on flood frequencies, as earlier studies have shown (Huang et al., 2017; Tian et al., 2017; Xing et al., 2018). The constant overestimation in this classification level of *permanently flooded wetland* was most likely due to the fact that this class is rare within the study area, while the size of its training sample was equal to the more abundant classes. Using such an equal-size training sample design usually leads to overestimations of rare classes (Colditz, 2015). An important note for the classifications in both Level 2 and Level 3 is that possible misclassified wetlands in Level 1 are included in these subsequent levels and may have caused extra confusion.

The overlaid outputs of all classification levels revealed maps that show both wetland vegetation types and surface water dynamics. In this way, results were presented for mapping wetland characteristics at a high resolution in multiple levels. The combination of Sentinel-1 and -2 reached OAs of 69.1% and 76.4% for mapping ten and seven multi-level wetland classes respectively (Table 5). Combining all levels into integrated maps naturally led to decreasing accuracies, because errors from all individual classification levels were transferred into the overlay.

It was found that the total extent of wetlands mapped in this study was rather similar to the extent mapped in earlier high-resolution general land cover classifications in the St. Lucia Wetlands (e.g. Ezemvelo KZN Wildlife, 2011; GTI, 2015). However, the presented multi-level classification method contributes largely by further characterising these wetlands for their vegetation types and surface water dynamics and reveals more detailed information beyond the general delineation of wetland extent. Although the presented methods in this study will be transferable for large scale mapping, their applicability to other climate zones should be assessed in further research.

A main limitation in this study was the collection process of training- and validation samples. Although the use of high-resolution aerial- and satellite images is a widely adopted method for this purpose (Lesiv et al., 2018), on-site collection of samples would contribute to more reliable reference data. The use of high-resolution images as a reference has a limitation for the number of distinguishable classes to be used in the classification scheme. Especially in the Level 3 classification, more details in characterising surface water dynamics may better reveal the capabilities of the temporally dense Sentinel-1 data. However, methods used in this study to employ temporal metrics obtained over an entire time series may not be suitable to characterise more detailed dynamics in wetland areas. Other methods (e.g. classifications of single images or time series analyses with more temporal detail) should be considered in such cases. Also, the spectral resolution of Sentinel-2 could be exploited in a better way by incorporating additional indices or individual band measures, of which especially the

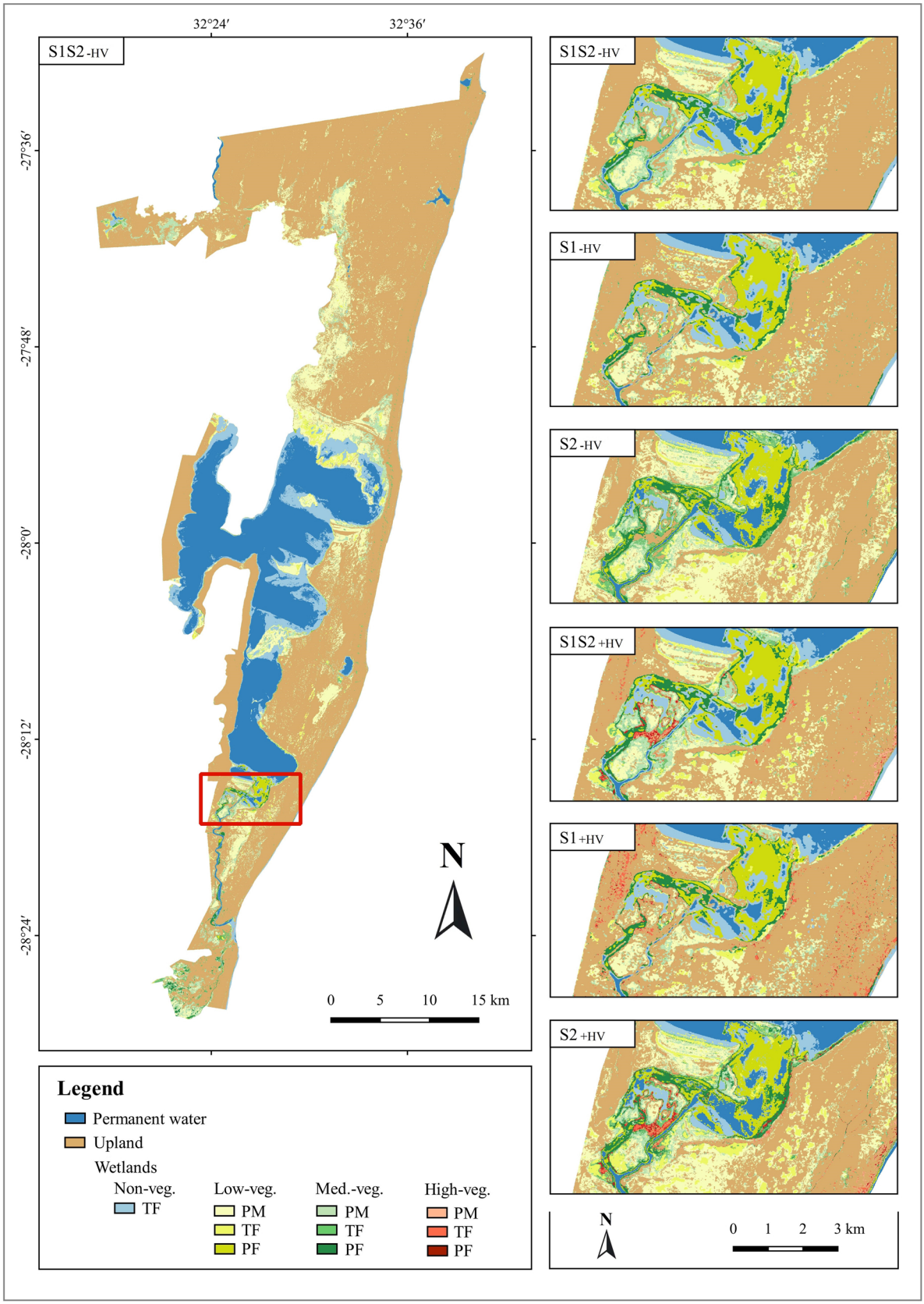

Fig. 7. Overlaid output of the $S1S2_{-HV}$ classification (left) and a detailed comparison of all overlaid outputs (right). PM = permanently moist, TF = temporarily flooded, PF = permanently flooded.

red-edge and NIR have an added value for wetland characterisation (Mahdavi et al., 2018).

6. Conclusion

The many different complexities occurring in wetlands make it challenging to characterise this valuable and threatened land cover type from space. This study presented the use of multitemporal Sentinel-1 and -2 data for comprehensive wetland characterisations. The use of the data was assessed in multiple levels including general wetland delineation, wetland vegetation types and surface water dynamics, which were applied in a sub-tropical study area. The results revealed high classification accuracies when combining Sentinel-1 and -2. Regarding the individual satellites, Sentinel-2 showed higher accuracies for general wetland delineation, while Sentinel-1 was preferred for mapping different wetland vegetation types. There were no significant accuracy differences for mapping surface water dynamics with either Sentinel-1 or -2. It was also found that mapping high-vegetated wetlands could not be done accurately, especially because Sentinel-1's C-band sensors in VV/VH mode did not suffice to detect subcanopy water bodies in flooded forests. When neglecting high-vegetated wetlands and using the combination of Sentinel-1 and -2, an OA of 76.4% was reached for a highly detailed wetland classification in the St. Lucia wetlands.

Regarding the current rates of wetland loss and the importance of wetland monitoring arising therefrom, this study contributed by revealing the potential of the freely available, high spatial and temporal resolution Sentinel-1 and -2 data for detailed, multi-level wetland characterisations. Given the limitations of this study, to improve the accuracy of wetland characterisation and to better characterise wetland dynamics, future studies may involve more sophisticated methods for time series analysis of Sentinel-1 and additional indices or band measurements of Sentinel-2. Besides this, on-site measurements to collect reference data will contribute largely to the accuracy assessments for this study.

Declaration of Competing Interest

The authors declare that they have no known competing financial interests or personal relationships that could have appeared to influence the work reported in this paper.

Acknowledgements

We thank Joost Brombacher from Wageningen University for his assistance with GEE scripting and Benjamin Kellenberger from Wageningen University for his advice on Random Forest parameters. We also thank the two anonymous reviewers for their helpful comments. This work contains modified Copernicus Sentinel-1 and -2 data (2014–2017). Planet data was provided through the Planet ambassador program.

References

Adam, E., Mutanga, O., 2009. Spectral discrimination of papyrus vegetation (Cyperus papyrus L.) in swamp wetlands using field spectrometry. ISPRS J. Photogramm. Remote Sens. 64, 612–620. https://doi.org/10.1016/j.isprsjprs.2009.04.004.

Amler, E., Schmidt, M., Menz, G., 2015. Definitions and mapping of east african wetlands: a review. Remote Sens. 7, 5256–5282. https://doi.org/10.3390/rs70505256.

Araya-López, R.A., Lopatin, J., Fassnacht, F.E., Hernández, H.J., 2018. Monitoring Andean high altitude wetlands in central Chile with seasonal optical data: A comparison between Worldview-2 and Sentinel-2 imagery. ISPRS J. Photogramm. Remote Sens. 145, 213–224. https://doi.org/10.1016/j.isprsjprs.2018.04.001.

Bassa, Z., Bob, U., Szantoi, Z., Ismail, R., 2016. Land cover and land use mapping of the iSimangaliso Wetland Park, South Africa: comparison of oblique and orthogonal random forest algorithms. J. Appl. Remote Sens. 10, 015017. https://doi.org/10.1117/1.jrs.10.015017.

Bhatnagar, S., Ghosh, B., Regan, S., Naughton, O., Johnston, P., Gill, L., 2018. Monitoring environmental supporting conditions of a raised bog using remote sensing techniques. Proc. IAHS 380, 9–15. https://doi.org/10.5194/piahs-380-9-2018.

Bourgeau-Chavez, L.K., Riordan, K., Powel, R., Miller, N., Nowels, M., 2009. Improving wetland characterization with multi-sensor, multi-temporal SAR and Optical/Infrared data fusion. Adv. Geosci. Remote Sens. https://doi.org/10.5772/8327.

Breiman, L., 2001. Random forests. Mach. Learn. 45, 5–32.

Cazals, C., Rapinel, S., Frison, P.-L., Bonis, A., Mercier, G., Mallet, C., Corgne, S., Rudant, J.-P., 2016. Mapping and characterization of hydrological dynamics in a coastal marsh using high temporal resolution Sentinel-1A images. Remote Sens. 8, 570. https://doi.org/10.3390/rs8070570.

Chatziantoniou, A., Petropoulos, G.P., Psomiadis, E., 2017. Co-Orbital Sentinel 1 and 2 for LULC mapping with emphasis on wetlands in a mediterranean setting based on machine learning. Remote Sens. 9, 1259. https://doi.org/10.3390/rs9121259.

Clulow, A.D., Everson, C.S., Price, J.S., Jewitt, G.P.W., Scott-Shaw, B.C., 2013. Water-use dynamics of a peat swamp forest and a dune forest in Maputaland, South Africa. Hydrol. Earth Syst. Sci. 17, 2053–2067. https://doi.org/10.5194/hess-17-2053-2013.

Colditz, R.R., 2015. An evaluation of different training sample allocation schemes for discrete and continuous land cover classification using decision tree-based algorithms. Remote Sens. 7, 9655–9681. https://doi.org/10.3390/rs70809655.

Copernicus Global Land Service, 2019. Copernicus Global Land Service- Land Cover. [WWW Document]. URL https://land.copernicus.eu/global/products/lc (Accessed 9.26.19). .

Di Gregorio, A., 2005. Land Cover Classification System: Classification Concepts and User Manual: LCCS. Food Agric. Organ, United Nations.

Drusch, M., Del Bello, U., Carlier, S., Colin, O., Fernandez, V., Gascon, F., Hoersch, B., Isola, C., Laberinti, P., Martimort, P., Meygret, A., Spoto, F., Sy, O., Marchese, F., Bargellini, P., 2012. Sentinel-2: ESA's optical high-resolution mission for GMES operational services. Remote Sens. Environ. 120, 25–36. https://doi.org/10.1016/j.rse.2011.11.026.

Ezemvelo KZN Wildlife, 2011. KwaZulu-Natal Land Cover 2008 V1.1. Unpublished GIS Coverage [Clp_KZN_2008_LC_V1_1_grid_w31.zip]. Pietermaritzburg. .

Farr, T.G., Rosen, P.A., Caro, E., Crippen, R., Duren, R., Hensley, S., Kobrick, M., Paller, M., Rodriguez, E., Roth, L., Seal, D., Shaffer, S., Shimada, J., Umland, J., Werner, M., Oskin, M., Burbank, D., Alsdorf, D.E., 2007. The shuttle radar topography mission. Rev. Geophys. 45. https://doi.org/10.1029/2005RG000183.

Federal Geographic Data Committee, 1997. National Vegetation Classification Standard.

Gallant, A.L., 2015. The challenges of remote monitoring of wetlands. Remote Sens. 7, 10938–10950. https://doi.org/10.3390/rs70810938.

GeoTerraImage, 2015. South African National Land-cover Dataset 2013–2014.

Google, 2018a. Sentinel-1 Algorithms. [WWW Document]. URL https://developers.google.com/earth-engine/sentinel1 (Accessed 11.11.18). .

Google, 2018b. Google Earth.

Gorelick, N., Hancher, M., Dixon, M., Ilyushchenko, S., Thau, D., Moore, R., 2017. Google earth engine: planetary-scale geospatial analysis for everyone. Remote Sens. Environ. 202, 18–27. https://doi.org/10.1016/j.rse.2017.06.031.

Gumbricht, T., Roman-Cuesta, R.M., Verchot, L., Herold, M., Wittmann, F., Householder, E., Herold, N., Murdiyarso, D., 2017. An expert system model for mapping tropical wetlands and peatlands reveals South America as the largest contributor. Glob. Change Biol. 23, 3581–3599. https://doi.org/10.1111/gcb.13689.

Henderson, F.M., Lewis, A.J., 2008. Radar detection of wetland ecosystems: a review. Int. J. Remote Sens. 29, 5809–5835. https://doi.org/10.1080/01431160801958405.

Hird, J.N., DeLancey, E.R., McDermid, G.J., Kariyeva, J., 2017. Google earth engine, open-access satellite data, and machine learning in support of large-area probabilistic wetland mapping. Remote Sens. 9, 1315. https://doi.org/10.3390/rs9121315.

Hoekman, D.H., Reiche, J., 2015. Multi-model radiometric slope correction of SAR images of complex terrain using a two-stage semi-empirical approach. Remote Sens. Environ. 156, 1–10. https://doi.org/10.1016/j.rse.2014.08.037.

Hu, S., Niu, Z., Chen, Y., 2017. Global wetland datasets: a review. Wetlands 37, 807–817. https://doi.org/10.1007/s13157-017-0927-z.

Huang, W., Devries, B., Huang, C., Jones, J., Lang, M., Creed, I., 2017. Automated extraction of inland surface water extent from sentinel-1 data. International Geoscience and Remote Sensing Symposium (IGARSS) 2259–2262. https://doi.org/10.1109/IGARSS.2017.8127439.

iSimangaliso Wetland Park Authority, 2017. iSimangaliso: The Restoration of Africa's Largest Estuarine Lake Receives a Boost. [WWW Document]. URL https://isimangaliso.com/newsflash/south-africas-largest-wetland-rehabilitation-project-achieves-important-milestone/ (Accessed 11.13.18). .

Kaplan, G., Avdan, U., 2018a. Sentinel-1 and Sentinel-2 data fusion for mapping and monitoring wetlands. Preprints. https://doi.org/10.20944/preprints201807.0244.v1.

Kaplan, G., Avdan, U., 2018b. Monthly analysis of wetlands dynamics using remote sensing data. ISPRS Int. J. Geo-Inf. 7, 411. https://doi.org/10.3390/ijgi7100411.

Kaplan, G., Avdan, U., 2017. Mapping and monitoring wetlands using Sentinel-2 satellite imagery. ISPRS Ann. Photogramm. Remote Sens. Spat. Inf. Sci. 4, 271–277. https://doi.org/10.5194/isprs-annals-IV-4-W4-271-2017.

Keddy, P.A., 2010. Wetland Ecology: Principles and Conservation. Cambridge University Presshttps://doi.org/10.1017/CBO9780511778179.

Kriegler, F.J., Malila, W.A., Nalepka, R.F., Richardson, W., 1969. Preprocessing transformations and their effects on multispectral recognition. Proceedings of the 6th International Symposium on Remote Sensing of Environment.

Lee, J.Sen, Ainsworth, T.L., Wang, Y., Chen, K.S., 2015. Polarimetric SAR speckle filtering and the extended sigma filter. IEEE Trans. Geosci. Remote Sens. 53, 1150–1160. https://doi.org/10.1109/TGRS.2014.2335114.

Lesiv, M., See, L., Laso Bayas, J., Sturn, T., Schepaschenko, D., Karner, M., Moorthy, I., McCallum, I., Fritz, S., 2018. Characterizing the spatial and temporal availability of very high resolution satellite imagery in google earth and microsoft Bing maps as a source of reference data. Land 7, 118. https://doi.org/10.3390/land7040118.

Lück-Vogel, M., Mbolambi, C., Rautenbach, K., Adams, J., Van Niekerk, L., 2016.

Vegetation mapping in the St Lucia estuary using very high-resolution multispectral imagery and LiDAR. South Afr. J. Bot. 107, 188–199. https://doi.org/10.1016/j.sajb.2016.04.010.
Ludwig, C., Walli, A., Schleicher, C., Weichselbaum, J., Riffler, M., 2019. A highly automated algorithm for wetland detection using multi-temporal optical satellite data. Remote Sens. Environ. 224, 333–351. https://doi.org/10.1016/j.rse.2019.01.017.
Mahdavi, S., Salehi, B., Granger, J., Amani, M., Brisco, B., Huang, W., 2018. Remote sensing for wetland classification: a comprehensive review. GIScience Remote Sens. 55, 623–658. https://doi.org/10.1080/15481603.2017.1419602.
Mahdianpari, M., Salehi, B., Mohammadimanesh, F., Homayouni, S., Gill, E., 2018. The first wetland inventory map of Newfoundland at a spatial resolution of 10 m using Sentinel-1 and Sentinel-2 data on the google earth engine cloud computing platform. Remote Sens. 11, 43. https://doi.org/10.3390/rs11010043.
Maseko, M.S.T., Ramesh, T., Kalle, R., Downs, C.T., 2017. Response of Crested Guineafowl (Guttera edouardi), a forest specialist, to spatial variation in land use in iSimangaliso Wetland Park, South Africa. J. Ornithol. 158, 469–477. https://doi.org/10.1007/s10336-016-1406-7.
Microsoft Bing Maps, 2018. Bing Maps.
Millennium Ecosystem Assessment, 2005. Ecosystems and Human Well-Being: Wetlands and Water. Washington DC. .
Mitsch, W.J., Gosselink, J.G., 2015. Wetlands, 5th edition. John Wiley & Sonshttps://doi.org/10.1002/ldr.3400050107.
Mleczko, M., Mróz, M., 2018. Wetland mapping using SAR data from the Sentinel-1A and TanDEM-X missions: a comparative study in the Biebrza Floodplain (Poland). Remote Sens. 10, 78. https://doi.org/10.3390/rs10010078.
Mróz, M., Mleczko, M., Fitrzyk, M., 2016. Exploitation of Sentinel-1a data in one year survey of water transfer on wetlands. Living Planet Symposium.
Mucina, L., Rutherford, M.C., Powrie, L.W., 2006. Vegetation Map of South Africa, Lesotho and Swaziland. South African Natl. Biodivers. Inst.
Muro, J., Canty, M., Conradsen, K., Hüttich, C., Nielsen, A.A., Skriver, H., Remy, F., Strauch, A., Thonfeld, F., Menz, G., 2016. Short-term change detection in wetlands using Sentinel-1 time series. Remote Sens. 8, 1–14. https://doi.org/10.3390/rs8100795.
National Geospatial Information (South Africa), 2018. Aerial Photography.
Nel, J.L., Murray, K.M., Maherry, A.M., Petersen, C.P., Roux, D.J., Driver, A., Hill, L., Van Deventer, H., Funke, N., Swartz, E.R., Smith-Adao, L.B., Mbona, N., Downsborough, L., Nienaber, S., 2011. Technical Report: National Freshwater Ecosystem Priority Areas Project. WRC Report No. 1801/2/11. Pretoria. .
Oshiro, T.M., Perez, P.S., Baranauskas, J.A., 2012. How many trees in a random forest? Machine Learning and Data Mining in Pattern Recognition. MLDM 2012. Lecture Notes in Computer Science, pp. 154–168. https://doi.org/10.1007/978-3-642-31537-4_13.
Ozesmi, S.L., Bauer, M.E., 2002. Satellite remote sensing of wetlands. Wetl. Ecol. Manag. 10, 381–402. https://doi.org/10.1023/A:1020908432489.
Pekel, J.-F., Cottam, A., Gorelick, N., Belward, A.S., 2016. High-resolution mapping of global surface water and its long-term changes. Nature 540, 418–422. https://doi.org/10.1038/nature20584.
Perissinotto, R., Stretch, D.D., Taylor, R.H., 2013. Ecology and Conservation of Estuarine Ecosystems: Lake St Lucia As a Global Model. Cambridge University Presshttps://doi.org/10.1017/CBO9781139095723.
Planet, 2018. Image Courtesy of Planet Labs, Inc.Image Courtesy of Planet Labs, Inc.
R Core Team, 2018. R: a Language and Environment for Statistical Computing.
Ramsar Convention, 2016. The 4th Strategic Plan 2016 – 2024. Gland, Switzerland. .
Rodriguez-Galiano, V.F., Ghimire, B., Rogan, J., Chica-Olmo, M., Rigol-Sanchez, J.P., 2012. An assessment of the effectiveness of a random forest classifier for land-cover classification. ISPRS J. Photogramm. Remote Sens. 67, 93–104. https://doi.org/10.1016/j.isprsjprs.2011.11.002.
Rosenqvist, A., Finlayson, C.M., Lowry, J., Douglas, T., 2007. The potential of long-wavelength satellite-borne radar to support implementation of the Ramsar Wetlands Convention. Aquat. Conserv. Mar. Freshw. Ecosyst. 17, 229–244.
Semeniuk, V., Semeniuk, C.A., 1997. A geomorphic approach to global classification for natural inland wetlands and rationalization of the system used by the Ramsar Convention – a discussion. Wetl. Ecol. Manag. 5, 145–158. https://doi.org/10.1023/A:1008207726826.
Shimada, M., Itoh, T., Motooka, T., Watanabe, M., Shiraishi, T., Thapa, R., Lucas, R., 2014. New global forest/non-forest maps from ALOS PALSAR data (2007–2010). Remote Sens. Environ. 155, 13–31. https://doi.org/10.1016/j.rse.2014.04.014.
Tian, H., Li, W., Wu, M., Huang, N., Li, G., Li, X., Niu, Z., 2017. Dynamic monitoring of the largest freshwater lake in China using a new water index derived from high spatiotemporal resolution sentinel-1A data. Remote Sens. 9, 6–9. https://doi.org/10.3390/rs9060521.
Tiner, R.W., 1999. Wetland Indicators: A Guide to Wetland Identification, Delineation, Classifcation, and Mapping. CRC Press LLC, Boca Raton. https://doi.org/10.1201/9781420048612.ch1.
Torres, R., Snoeij, P., Geudtner, D., Bibby, D., Davidson, M., Attema, E., Potin, P., Rommen, B.Ö., Floury, N., Brown, M., Traver, I.N., Deghaye, P., Duesmann, B., Rosich, B., Miranda, N., Bruno, C., L'Abbate, M., Croci, R., Pietropaolo, A., Huchler, M., Rostan, F., 2012. GMES Sentinel-1 mission. Remote Sens. Environ. 120, 9–24. https://doi.org/10.1016/j.rse.2011.05.028.
Tsendbazar, N.E., de Bruin, S., Mora, B., Schouten, L., Herold, M., 2016. Comparative assessment of thematic accuracy of GLC maps for specific applications using existing reference data. Int. J. Appl. Earth Obs. Geoinf. 44, 124–135. https://doi.org/10.1016/j.jag.2015.08.009.
Tsyganskaya, V., Martinis, S., Marzahn, P., Ludwig, R., 2018. Detection of temporary flooded vegetation using Sentinel-1 time series data. Remote Sens. 10, 1286. https://doi.org/10.3390/rs10081286.
Wang, Y., Hess, L.L., Filoso, S., Melack, J.M., 1995. Understanding the radar backscattering from flooded and nonflooded Amazonian forests: results from canopy backscatter modeling. Remote Sens. Environ. 54, 324–332. https://doi.org/10.1016/0034-4257(95)00140-9.
Whyte, A., Ferentinos, K.P., Petropoulos, G.P., 2018. A new synergistic approach for monitoring wetlands using Sentinels -1 and 2 data with object-based machine learning algorithms. Environ. Model. Softw. 104, 40–54. https://doi.org/10.1016/j.envsoft.2018.01.023.
Xing, L., Tang, X., Wang, H., Fan, W., Wang, G., 2018. Monitoring monthly surface water dynamics of Dongting Lake using Sentinal-1 data at 10 m. PeerJ 6. https://doi.org/10.7717/peerj.4992.
Xu, H., 2006. Modification of normalised difference water index (NDWI) to enhance open water features in remotely sensed imagery. Int. J. Remote Sens. 27, 3025–3033. https://doi.org/10.1080/01431160600589179.